Control of the high-order harmonics cutoff and attosecond pulse generation through the combination of a chirped fundamental laser and a subharmonic laser field

Jie Wu, Gang-Tai Zhang, Chang-Long Xia, and Xue-Shen Liu*

Institute of Atomic and Molecular Physics, Jilin University, Changchun 130012, People's Republic of China

(Received 1 November 2009; revised manuscript received 31 March 2010; published 19 July 2010)

We propose a method to generate an isolated attosecond (as) pulse in combination with a chirped fundamental laser field (5 fs, 800 nm) and a subharmonic laser field (12 fs, 1600 nm). It is shown that, for the case of the chirped parameter $\beta = 0.25$, not only is the efficiency of the extended harmonics enhanced, but also an ultrabroad supercontinuum is formed in the second plateau. For the case of $\beta = 0.65$, an ultrabroad supercontinuum spectrum with the width of about 1670 eV can be observed. Furthermore, due to the introduction of chirped pulse, the short quantum trajectory is enhanced, and the long one is suppressed. By superposing a properly selected range of the harmonic spectrum in the continuum region, an intense isolated 38-as pulse is generated.

DOI: 10.1103/PhysRevA.82.013411 PACS number(s): 32.80.Rm, 42.50.Hz, 42.65.Ky

Attosecond (as) metrology will open new fields of time-resolved studies with unprecedented resolution [1–3]. Just as femtosecond pulses have provided a natural time scale of electronic motion in a mean-field potential of solids and molecules, as pulses are important tools for studying and controlling the motion of electrons inside atoms and molecules. Such examples are controlling molecular motion [4], exciting inner-shell electrons [5], tracing motion of bound electrons [6], and above-threshold ionization [7,8].

So far, experimentally high-order harmonic generation (HHG), a phenomenon that occurs in multiphoton physics when atoms or molecules are driven by short intense laser pulses [9], has been the most advanced method that can produce single as pulses. Moreover, for its potential applications, such as obtaining a coherent light in the extreme ultraviolet [10–12] and obtaining a coherent soft x-ray source [13–15], research on HHG has rapidly advanced in the past decade. Both experimental and theoretical studies have shown that an HHG spectrum has a general character: It decreases rapidly for the first few harmonics, then exhibits a broad plateau, and finally ends up with a sharp cutoff. An HHG process can be well understood by means of the well-known semiclassical three-step model [16–19] and by full quantum theory [20]. First, an electron tunnels through the barrier that is formed by the Coulomb potential and the laser field. Second, the electron oscillates and gains kinetic energy under the influence of the laser field. Finally, when the laser field inverses its direction, the electron is pulled back to recombine with the parent ion and emits a harmonic photon. In an oscillating field, this process repeats every half cycle; under a multicycle driving pulse, this will lead to a train of as pulses with a periodicity of half an optical cycle. However, for practical applications, as metrology prefers an isolated as pulse. Hence, obtaining an isolated as pulse with a shorter duration has been a common goal of research in recent years [21,22].

From the three-step model, we can see that an HHG process can be controlled at different stages. By choosing a two-color field, the electron motion in the second stage of the three-step model, as well as the HHG process, can be controlled. Mauritsson *et al.* [23] have studied as-pulse generation by using two-color laser fields. Zeng *et al.* [11] have theoretically obtained an ultrabroad extreme ultraviolet supercontinuum spectrum with the spectral width of 148 eV, which has directly created an isolated 65-as pulse by using a two-color laser field. However, due to the inherent characteristic of the two-color scheme, the efficiency of the continuous harmonics is low, which directly affects the intensity of the as pulse and its applications. A great amount of effort has been devoted to enhance the harmonic efficiency. Watson *et al.* [24] have demonstrated that a coherent superposition state can induce a dipole transition between the continuum and the ground state via an excited state responsible for the ionization. Thus, the conversion efficiency of HHG can be improved by choosing the superposition state as the initial state [25,26]. By combining the coherent superposition and the two-color laser field with a suitably adjusted relative phase between the two pulses [27], the high harmonic efficiency can be enhanced efficiently, and an intense isolated 45-as pulse can be obtained.

Moreover, controlling quantum trajectories is a useful method for generating an isolated as pulse [28]. It has been shown that there are two paths, the so-called long path and short path, which contribute to every harmonic. Because the two paths have different emission times, the harmonics are not phase locked [29]. As a result, properly superposing a range of harmonic spectra leads to an irregular as pulse with two separate bursts. To resolve this problem, it is essential to control the quantum path so as to pick out one single path and filter several consecutive harmonics in the cutoff region. Superposition of consecutive harmonics can yield an as pulse, provided that these harmonics are in phase. However, propagation effects may play an important role in influencing the harmonics. Under appropriate conditions, the short trajectories may be selected by propagation effects, and the time confinement of as pulses can be improved [13].

In order to control quantum paths of high-order harmonics and as-pulse generation, Hong *et al.* [30] have studied high-order harmonics and as-pulse generation in the presence of a static electric field. Moreover, the laser parameters directly affect the electron motion and the HHG process. With the introduction of a chirp, the symmetry of the fundamental laser field is destroyed by changing its frequency, period, wavelength, and the laser peak. The electron motion can also be changed correspondingly. Hence, the plateau of the

*liuxs@jlu.edu.cn

harmonic spectrum can be broadened by properly choosing the chirp parameters. Furthermore, high harmonics emitted by many-cycle pulses may not be synchronized on an as time scale, which sets a lower limit on the achievable x-ray pulse duration [31]. However, the dynamically induced harmonic chirp can be compensated by introducing an appropriately designed frequency chirp on the laser beam [32]. Carrera and Chu [33] have used a hyperbolic tangent chirped laser field to remarkably extend the cutoff position of the harmonic spectrum. Xiang *et al.* [34] have studied the control of the high-order harmonics cutoff by combining a chirped laser with a static electric field and have obtained an isolated 10-as pulse.

Although the effects of two-color laser field, chirped laser field, and coherent superposition of states, respectively, have been investigated, so far, no study has been reported for the combination of these effects. Here, we wish to determine what would happen if this combination of superposition of states, two-color field, and chirped fundamental laser field is adopted. Very recently, it has been theoretically demonstrated that an isolated 26-as pulse can be obtained when a model He^+ ion is exposed to the combination of an intense few-cycle chirped laser pulse and its 27th harmonics [35]. Zou *et al.* [36] have investigated the coherent control of broadband isolated as pulses in a chirped two-color laser field.

Our calculations have indicated that the emission from a superposition state differs from the emission from an excited or the ground state. When the initial state is prepared as a coherent superposition of the ground and the first excited states, the conversion efficiency for harmonic generation can be greatly enhanced in comparison with the case where the initial state is prepared in the ground state or the first excited state. These results are consistent with those reported by Sanpera *et al.* [26]. Moreover, there is interference between the ground state and the excited state, as investigated by Sanpera *et al.* [26]. However, the present paper will focus on topics such as how to increase the conversion efficiency and how to extend the plateau of harmonic spectrum, what are the effects of the two-color laser field as well as the superposition of states and the chirp, and how these parameters affect the HHG process. No intention has been made to discuss issues that involve interference between states.

In this paper, we study the control of high-order harmonics cutoff and as-pulse generation by combining a chirped fundamental laser with a subharmonic laser field by using a coherent superposition of the ground state and the first excited state as the initial state. Although the phase difference between the component states is adjustable, for the sake of simplicity, we set it to be zero in our work [24–26]. With the introduction of the chirped parameter, the trajectories of the electron wave packet are modified, the short quantum trajectory is enhanced, the long quantum trajectory is suppressed, and the cutoff position of the harmonics can be remarkably extended. By adjusting the chirped parameter, an ultrabroad supercontinuum with the width of 1670 eV can be obtained. By superposing a properly selected range of harmonic spectrum in the continuum region, an intense isolated 38-as pulse can be generated. To explore the underlying mechanism responsible for the enhancement of the harmonic efficiency and the cutoff extension, we perform time-frequency analysis of emitted pulses by means of the wavelet transform of the induced dipole acceleration and a classical simulation based on the three-step model.

We investigate the HHG and as-pulse generation by numerically solving the time-dependent Schrödinger equation for a one-dimensional model He^+ ion with the help of the splitting-operator fast-Fourier transform technique. We choose the soft-core Coulomb potential $V(x) = -a/\sqrt{x^2+b}$ for He^+. We set soft-core parameters to be $a = 2$ and $b = 0.5$, which can reproduce the ground-state binding energy 2.0 a.u. for He^+. In our simulation, a chirped 5-fs, 800-nm fundamental laser field and a subharmonic 12-fs, 1600-nm laser field are combined to serve as the driving pulse for generating as pulses. The expression of the synthesized field can be written as $E(t) = E_0 f_0(t)\sin[\omega_0 t + \delta(t)] + E_1 f_1(t)\sin(\omega_1 t)$, where E_i $(i = 0,1)$ are the amplitudes of the laser fields, $f_i(t) = \exp[-4\ln(2)(t - T_0/2)^2/\tau_i^2]$ $(i = 0,1)$ are the laser field envelopes, and ω_i and τ_i $(i = 0,1)$ are the corresponding frequencies and the durations of the laser fields. Furthermore, $\delta(t)$ is the carrier-envelope phase, which has the time-varying form $\delta(t) = -\beta\omega_0 t^2/T_0$. The chirp form is controlled by adjusting the two parameters β and T_0. In our paper, however, we fix T_0 to be 36 fs, the length of time for the time evolution. Due to recent advances in comb laser technology, it is highly likely that such a laser is achievable in the near future. It is noted that the use of linear chirping is a more practical measure to ensure experimental feasibility [37].

We first consider the case where the parameters for the synthesized chirped fundamental laser field are (5 fs, 800 nm, $\beta = 0.25$), and the parameters for the subharmonic laser field are (12 fs, 1600 nm). The harmonic spectrum is shown in Fig. 1 (the red dotted curve). For comparison, we also present the harmonic spectrum in the two-color laser field without chirping, as shown in Fig. 1 (the black solid curve). We

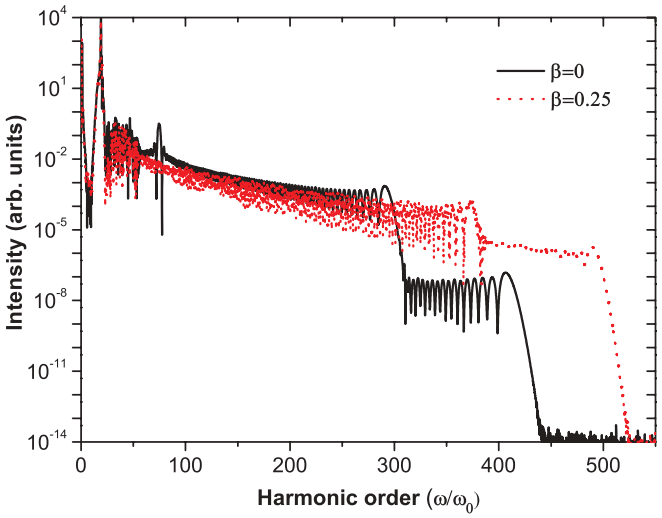

FIG. 1. (Color online) The black solid curve: harmonic spectrum of the He^+ ion generated by the two-color laser field synthesized by a fundamental laser field (5 fs, 800 nm) without chirp and a subharmonic laser field (12 fs, 1600 nm). The red dotted curve: harmonic spectrum of the He^+ ion generated by the synthesized chirped fundamental laser field (5 fs, 800 nm, $\beta = 0.25$) and the subharmonic laser field (12 fs, 1600 nm).

calculated the harmonic spectrum and the generation of as pulses under different laser field intensities and found that, in a certain intensity range (below the ionization saturated intensity), the numerical results have similar features. Thus, in this paper, we chose the intensities of the fundamental and the subharmonic laser fields as 1×10^{15} and 2×10^{14} W/cm^2, respectively. As shown in Fig. 1, the harmonic spectra for both cases show a similar structure with two plateaus; but the two cutoff positions of the spectrum, for the case of the chirped two-color laser field, are extended from the 290th and the 405th order of the two-color laser field without chirp to the 372nd and the 485th order, respectively. Although the width of the second plateau in the two cases is almost the same, the efficiency for the chirped second plateau, which is much smoother without large modulation, is about 2 orders of magnitude higher than that without chirp.

To further understand the harmonic spectral characteristics and the difference between the two spectra, we studied the time-frequency distributions of HHG by using the wavelet transformation of the dipole acceleration [38]. The results are shown in Figs. 2(a) and 2(b). From the time-frequency analysis, we can obtain information on the emission times of the photons with different photon energies. As shown in Fig. 2, there are two photon-energy peaks, which are labeled as A_1, A_2 and B_1, B_2 for each laser field. The two peaks indicate the recombination times as well as the maximum kinetic energies of the electrons that return to their parent ions. We can also see that the heights and the intensities of the two emission peaks are different in each case. From Fig. 2(b), it can be seen that, for the case of the chirped two-color laser field ($\beta = 0.25$), the heights of peaks B_1 and B_2 are higher than those in Fig. 2(a), which demonstrates the extension of the cutoff positions of the harmonic spectra. In addition, the intensities of A_2 and B_2 are stronger than those of A_1 and B_1, respectively, which indicates the existence of a double-plateau structure and explains why the second plateau is lower than the first one. Except from those mentioned previously, from Figs. 2(a) and 2(b), we can see that, there are two dominant quantum paths with different emission times that contribute to each harmonic in each optical cycle. The positive-slope section (the down-side part of each peak) and the negative-slope section (the up-side part of each peak) correspond to the so-called short trajectory and long trajectory, respectively. For the case of the two-color laser field, the two trajectories that construct peak A_1 are almost the same. However, when the chirp is introduced, the intensity of the short trajectory is enhanced, which explains why the second plateau is higher in the latter (with chirping) than in the former (without chirping). In addition, due to the enhancement of the short trajectory, the interference between the short and long trajectories decreases, which means that there is a small modulation in the second plateau for the case $\beta = 0.25$.

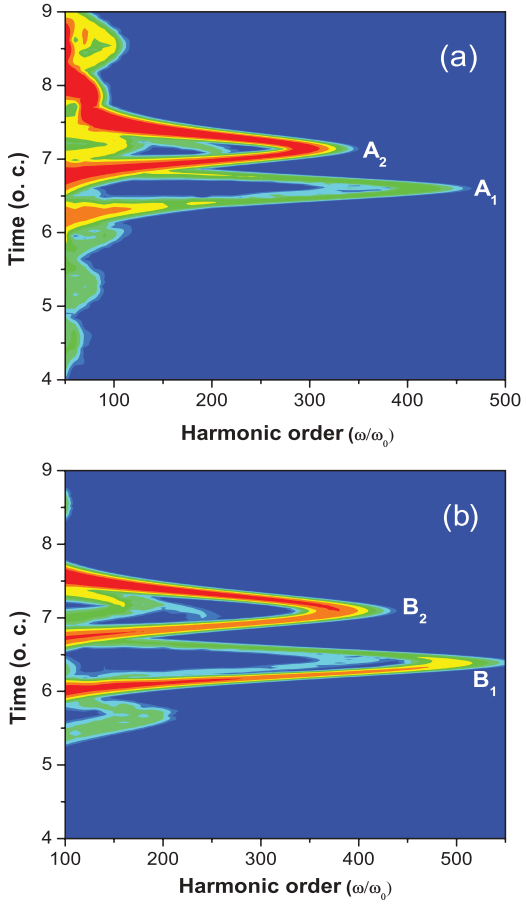

FIG. 2. (Color online) The time-frequency distribution of the HHG spectra that corresponds to the (a) black solid curve and (b) the red dotted curve in Fig. 1. The laser parameters are the same as those in Fig. 1. o.c. denotes optical cycle.

Now, we consider the generation of as pulses from HHG for $\beta = 0$ and $\beta = 0.25$, respectively. The temporal profile is obtained by superposing several orders of the harmonics [30]. First, we illustrate the temporal profiles of the as pulses for the case $\beta = 0$. By superposing 105 harmonics, which range from the 300th to the 405th order in the second plateau, an irregular as pulse with two main bursts in one cycle is observed as shown in Fig. 3(a). By superposing 55 harmonics from the 350th to the 405th order in the second plateau, a regular as-pulse train with two bursts in each cycle is observed as shown in Fig. 3(b). There are two trajectories that contribute to each harmonics in the second plateau, and these harmonics are not emitted in phase. Superposition of more harmonics would lead to a more irregular as-pulse train [31]. This kind of poor quality of as-pulse train will limit its application. Next, we present the temporal profiles of the as pulses for the case $\beta = 0.25$. By superposing 105 harmonics from the 380th to the 485th order in the second plateau, a much regular as pulse with only one main burst in each cycle is generated as shown in Fig. 3(c), together with some satellite pulses around it. The intensity of the pulse is about 2 orders of magnitude higher than that in the case of $\beta = 0$. This is because the short trajectory is enhanced, and the efficiency of the harmonic spectrum is increased by about 2 orders of magnitude. When we superpose a range of harmonic spectrum (e.g., from the 400th to the 450th order), an isolated regular as pulse with the duration of about 52 as can be generated, as shown in Fig. 3(d).

Next, we consider the case where the chirped parameter $\beta = 0.65$ but the other parameters are kept the same as those mentioned earlier. The harmonic spectrum is shown in Fig. 4(a) (the solid red curve). In order to give numerical information about the effects of the second laser intensity,

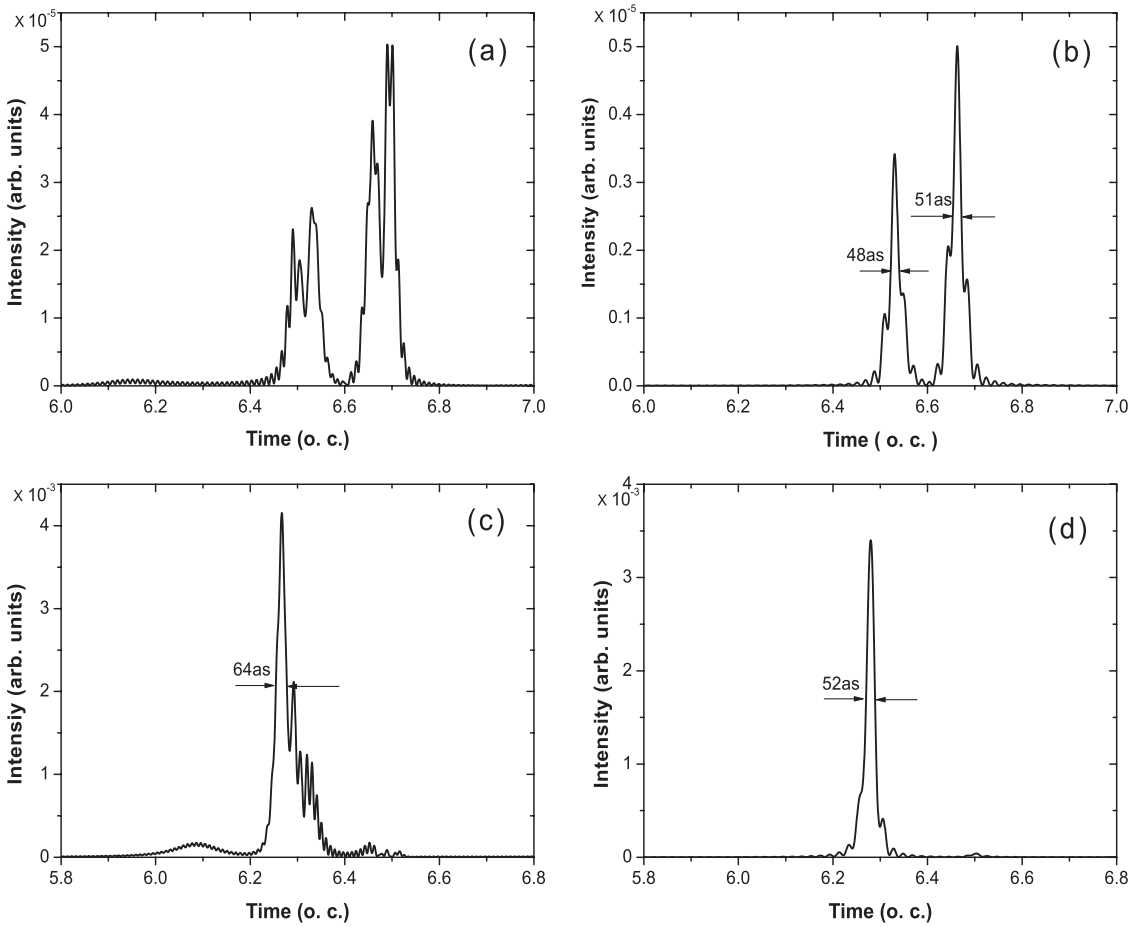

FIG. 3. (a) and (b) are the temporal profiles of the as pulses generated by superposing the harmonics from the 300th to the 405th order and from the 350th to the 405th order, respectively, for the case of the two-color laser field without chirping ($\beta = 0$). (c) and (d) are the temporal profiles of the as pulses generated by superposing the harmonics from the 380th to the 485th order and from the 400th to the 450th order, respectively, for the case of the chirped two-color laser field ($\beta = 0.25$). o.c. denotes optical cycle.

the harmonic spectrum with the intensity of the second field 6×10^{13} W/cm^2 is also presented in Fig. 4(a) (the black dotted curve). The solid red curve in Fig. 4(a) shows that, in this case, the double-plateau structure disappears (i.e., only one plateau exists), but the efficiency of the spectrum decreases with increasing harmonic order. The cutoff position of the harmonic plateau is extended to the 1314th order, by corresponding to the energy $I_P + 17.5U_P^{'}$ (1996 eV), where $U_P^{'} = E_0^2/(4\omega_0^2) + E_1^2/(4\omega_1^2)$ is the ponderomotive energy for the two-color case. At the same time, a supercontinuum with the spectral width of 1670 eV is formed from the 220th to the 1314th order. Figure 4(b) shows the corresponding time-frequency distribution of the HHG in Fig. 4(a) (the solid red curve). It can be seen that, for harmonics above the 220th order, there is only one trajectory, which contributes to the harmonic generation, whereas the long trajectory is completely suppressed. In this case, a supercontinuum is formed, which is beneficial to generate an intense isolated as pulse.

We present the temporal profiles of the as pulses for the case of the chirped parameter $\beta = 0.65$ in Fig. 5. Figure 5(a) shows that an isolated 59-as pulse, with one main burst in each cycle, but with some satellite pulses around it, is observed by superposing harmonics from the 250th to the 1300th order. This is because the temporal drift in harmonic emission has dramatic influence on the duration of the emitted as pulses, and high harmonics are not synchronized on an as time scale. The selection of an entire available spectral range no longer provides the shortest possible pulse [31]. Moreover, since there is only one trajectory that contributes to each harmonic, the generation of a regular isolated as pulse is possible by superposing a properly selected range of harmonic spectra. Figure 5(b) shows that an isolated as pulse with the duration of 48 as is observed by superposing 50 harmonics from the 1200th to the 1250th order near the cutoff, but the pulse intensity is very low. By superposing 50 harmonics from the 250th to the 300th order, an isolated as pulse with the same duration can be generated, and the intensity of the burst is enhanced by 5 orders of magnitude, as shown in Fig. 5(c). In addition, by superposing 70 harmonics from the 350th to the 420th order, an isolated regular as pulse with duration 38 as can be generated, as shown in Fig. 5(d).

In order to have a qualitative insight into the extension of the cutoff position of the harmonic spectrum, we analyze an HHG process by applying the semiclassical three-step model [16–20]. In this process, the motion of an electron

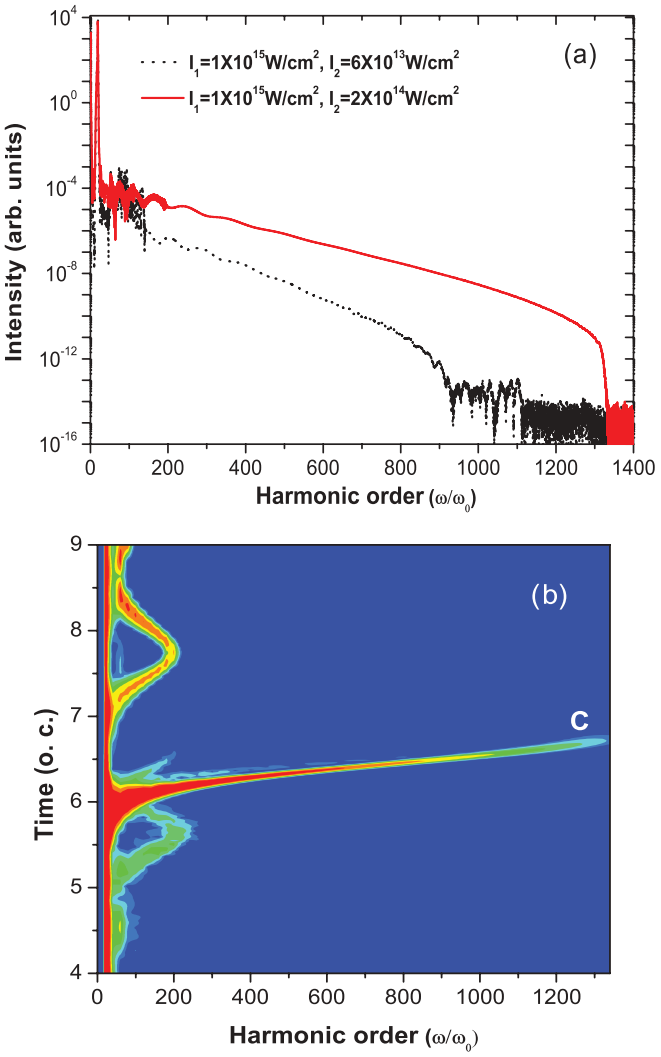

FIG. 4. (Color online) (a) Harmonic spectra of the He^+ ion generated by synthesizing the chirped fundamental laser field ($\beta = 0.65$) and the subharmonic laser field. (b) The corresponding time-frequency distribution of the HHG spectrum in (a) (the solid red curve). o.c. denotes optical cycle.

under the effective barrier formed by the ion and the laser field is described by the equation,

$$\ddot{x}(t) = -E(t),$$

where $E(t)$ is the laser field. By assuming that the initial velocity of the electron ionized from the parent ion is zero at t_i, we have

$$\dot{x}(t) = \int_{t_i}^{t} -E(t)dt,$$

and

$$x(t) = \int_{t_i}^{t} \dot{x}(t)dt.$$

If the electron is ionized at t_i, the corresponding emission time t_e can be obtained by solving the equation,

$$x(t_e) = \int_{t_i}^{t_e} \dot{x}(t)dt = 0.$$

The maximum kinetic energy E_k of the electron, which is ionized at t_i and returns to the parent ion at t_e, can be expressed as

$$E_k = \frac{1}{2}\left[\int_{t_i}^{t_e} -E(t)\,dt\right]^2.$$

The maximum photon energy is $I_p + E_k$.

Figure 6(a) shows the electric-field strength of a two-color laser field without chirping ($\beta = 0$); Fig. 6(b) shows the corresponding time dependence of the photon kinetic energy on the ionization (the blue trigonal curve) and the emission (the red circular curve) times. As shown in Fig. 6(b), most electrons are emitted mainly near the peaks marked as A_{i1} (5.0 o.c.) and A_{i2} (6.35 o.c.); they return to the parent ion at about A_{e1} (6.6 o.c.) and A_{e2} (7.1 o.c.) with maximum kinetic energies of 558 and 387 eV, respectively. The values of $I_p + 558$ and $I_p + 387$ eV roughly agree with the cutoff energies of the second plateau (405th order) and the first plateau (290th order) shown in Fig. 1 (the black solid curve). Furthermore, harmonic photons with the same energy greater than $I_p + 387$ eV are emitted at different times that correspond to the two electron trajectories. A trajectory with later ionization time but earlier emission time is called the short trajectory, and a trajectory with earlier ionization time but later emission time is called the long trajectory. As the kinetic energy increases, the emission time of short trajectory increases, and the emission time of the long trajectory decreases. Thus, these two emission times finally become equal at the maximum kinetic energy. The semiclassical analysis shown in Fig. 6(b) is qualitatively consistent with the time-frequency characteristic shown in Fig. 2(a).

By adding a chirp to the fundamental laser field, the electron dynamics can be modulated. Figure 6(c) shows the driving laser field for the case of $\beta = 0.25$, and Fig. 6(d) shows the corresponding time dependence of the photon energy on the ionization (the blue trigonal curve) and the emission (the red circular curve) times. It can be seen that most electrons are also emitted near two peaks, ionized at B_{i1} (5.3 o.c.) and B_{i2} (6.15 o.c.), and returned to the emitted photon energies at about B_{e1} (6.4 o.c.) and B_{e2} (7.1 o.c.), respectively. It is evident that the two peaks increase up to 682 and 511 eV, which corresponds to the second cutoff position (485th order) and the first cutoff position (372nd order), respectively, as shown in Fig. 1 (the red dotted curve). Although the energy difference between the two peaks is almost the same as that for the case $\beta = 0$, the maximum is enhanced for the case of $\beta = 0.25$.

Figure 7(a) presents the electric-field strength for the case of $\beta = 0.65$, which corresponds to a relatively high chirped parameter. In this case, the electron trajectories have been changed more remarkably, and some trajectories have been suppressed. As shown in Fig. 7(b), most electrons are ionized at about 4.9 o.c. and returned at about 6.8 o.c.. The long trajectory that contributes to the harmonics with the kinetic energies between 274 and 1942 eV has been suppressed; only the short trajectory contributes to these harmonics. This means that a broad supercontinuum harmonic plateau and an isolated intense as pulse can be obtained.

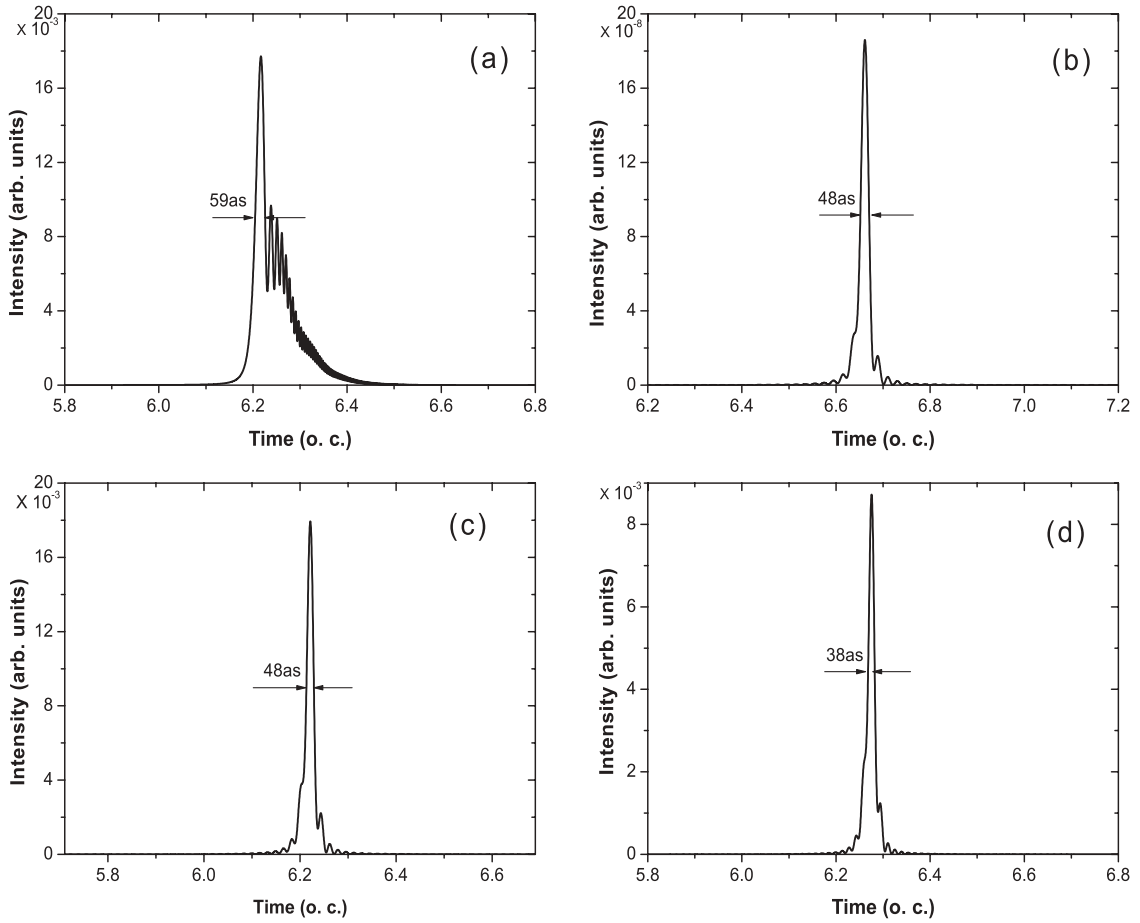

FIG. 5. The temporal profiles of the as pulses in the synthesized chirped fundamental laser field ($\beta = 0.65$) and the subharmonic laser field. (a) as pulse by superposing harmonics from the 250th order to the 1300th order. (b) as pulse by superposing harmonics from the 1200th order to the 1250th order. (c) as pulse by superposing harmonics from the 250th order to the 300th order. (d) as pulse by superposing harmonics from the 350th order to the 420th order. o.c. denotes optical cycle.

Furthermore, it has been pointed out that when the ionized electron spends a long time in the field, the spreading of the electron wave packet leads to a strong decrease in the harmonic efficiency [39]. Based on this idea, from Figs. 6(a) and 6(b), we can see that the electrons ionized at peak A_{i1} need about 1.6 o.c. to return to the parent ion; but the electrons ionized at peak A_{i2} need only 0.75 o.c. to recombine with the parent. In addition, all the electrons ionized around peak A_{i1} need much longer times to recombine with the parent ion. Therefore, the intensities of these harmonic spectra emitted around peak A_{e1} [or A_1 in Fig. 2(a)] are much lower than those around peak A_{e2} [or A_2 in Fig. 2(a)], which results in a double-plateau structure. For the case of $\beta = 0.25$, as shown in Figs. 6(c) and 6(d), the difference in returning time of the ionized electrons between peaks B_{i1} and B_{i2} is very small. Hence, the difference in harmonic spectral efficiency between the emission peaks B_{e1} and B_{e2} should become small. Indeed, from the time-frequency profile of Fig. 2(b) and the harmonic spectrum of Fig. 1 (the red dotted curve), we can see that the second plateau is enhanced. In addition, for the short trajectory between peaks B_{i1} and (B_{e1}), as well as B_{i2} and (B_{e2}), the return times of these electrons are evidently smaller in comparison with the case where there is no chirping. This explains the enhancement of the short trajectory that contributes to the emission peak B_1 in Fig. 2(b). For the case of $\beta = 0.65$, as shown in Fig. 7(b), when the harmonic order increases, the electron return time increases, which results in a decrease in harmonic efficiency, which is consistent with the harmonic spectrum in Fig. 4(a) and the corresponding time-frequency profile in Fig. 4(b).

According to the Ammosov-Delone-Krainov theory, the tunnel ionization rate is determined by $\exp[-4I_P\sqrt{2I_P}/3/|E(t)|]$ [40], which depends exponentially on the electric field. As shown in Fig. 6(a), the intensity of the laser field around peak A_{i1} is clearly lower than that around peak A_{i2}, and the ionized electrons near peaks A_{i1} and A_{i2} contribute to the second and first harmonic spectral plateaus, respectively. Hence, the harmonic spectral efficiency is lower in the second plateau. By introducing chirping, the laser field is changed, as shown in Fig. 6(c); specifically, the intensity of peak B_{i1} is about 42% higher in comparison with the situation where no chirping is presented, but the intensity of peak B_{i2} stays almost the same. Hence, the efficiency of the harmonic spectrum in the second plateau is enhanced. The difference in the efficiency between the two plateaus becomes small. For the case of $\beta = 0.65$, the electrons are mainly emitted around peak C_{i1}. We can see from Fig. 7(b) that, the earlier the ionization

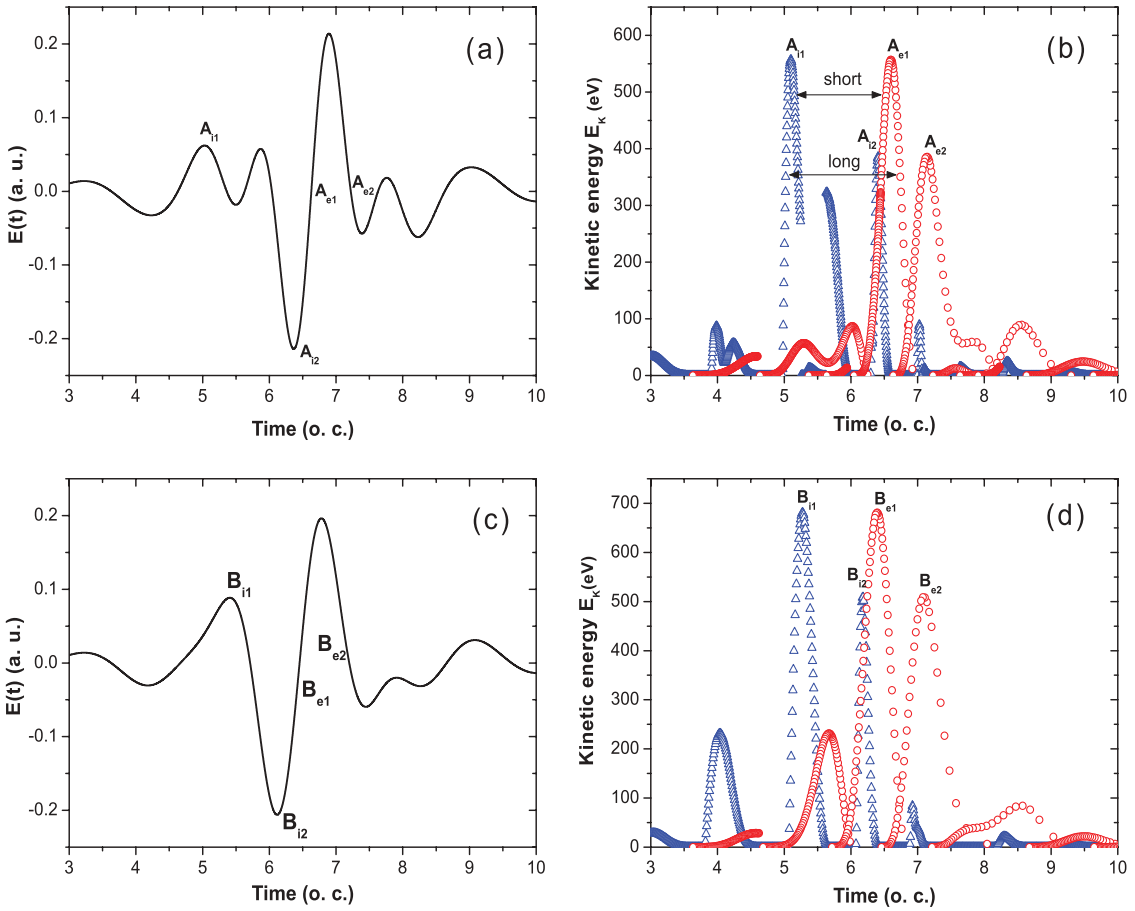

FIG. 6. (Color online) Electric field strength of the two-color laser field (a) without chirping ($\beta = 0$) and (c) with chirping ($\beta = 0.25$). (b) and (d) are the corresponding dependence of the harmonic order on the ionization time (the blue trigonal curve) and the emission time (the red circular curve). o.c. denotes optical cycle.

occurs, where the corresponding laser intensity is weaker, the higher the kinetic energy of the electron gets. Therefore, the efficiency of the harmonic spectrum gradually decreases as the harmonic order increases. These results agree with what we have discussed previously.

In conclusion, we have investigated the HHG and the generation of as pulses in combination with a chirped fundamental laser field and a subharmonic laser field. Our results have shown that, with the introduction of chirping, not only can the cutoff position of the harmonic spectrum be broadened, but

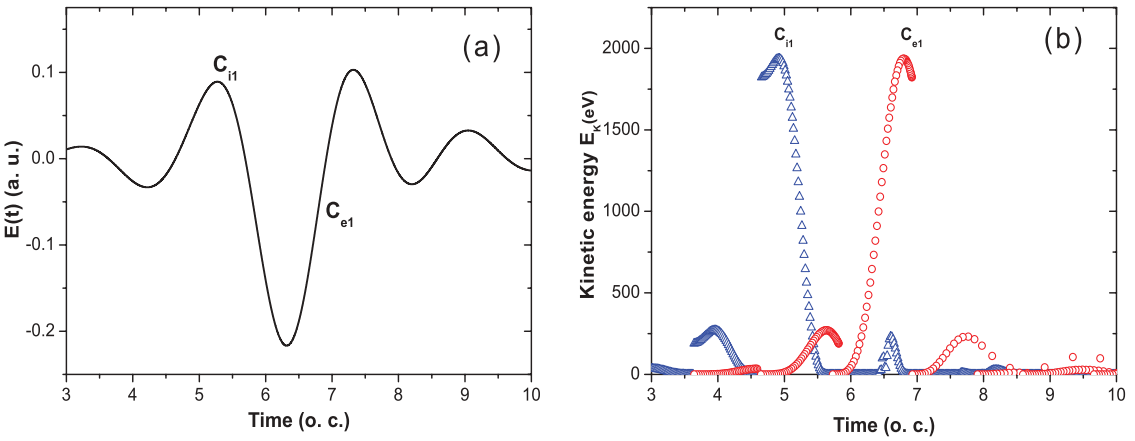

FIG. 7. (Color online) (a) Electric-field strength of the two-color laser field with the chirped parameter ($\beta = 0.65$). (b) The corresponding dependence of the harmonic order on the ionization time (the blue trigonal curve) and the emission time (the red circular curve). o.c. denotes optical cycle.

also the efficiency of the second plateau can be enhanced. To explain these results, we have analyzed the process of HHG by the semiclassical model. Moreover, by adding a chirp, the quantum paths in HHG can be controlled, and an isolated as can be obtained. By adjusting the chirped parameter, an ultrabroad supercontinuum with the width of 1670 eV has been observed. By superposing a proper range of harmonics in the supercontinuum, we have obtained an intense isolated 38-as pulse.

ACKNOWLEDGMENTS

We want to thank Z.-C. Yan for his critical reading of the manuscript. This work was supported by the National Natural Science Foundation of China under Grant No. 10974068.

[1] P. M. Paul, E. S. Toma, P. Breger *et al.*, Science **292**, 1689 (2001).
[2] A. L. Cavalieri, N. Müller, T. Uphues *et al.*, Nature (London) **449**, 1029 (2007).
[3] E. Goulielmakis, V. S. Yakovlev, A. L. Cavalieri *et al.*, Science **317**, 769 (2007).
[4] H. Niikura, F. Légaré, R. Hasbani *et al.*, Nature (London) **417**, 917 (2002).
[5] M. Drescher, M. Hentschel, R. Kienberger *et al.*, Nature (London) **419**, 803 (2002).
[6] M. Hentschel, R. Kienberger, C. Spielmann *et al.*, Nature (London) **414**, 509 (2001).
[7] P. Johnsson, R. López-Martens, S. Kazamias *et al.*, Phys. Rev. Lett. **95**, 013001 (2005).
[8] Y. Xiang, Y. Niu, and S. Gong, Phys. Rev. A **80**, 023423 (2009).
[9] N. A. Papadogiannis, B. Witzel, C. Kalpouzos, and D. Charalambidis, Phys. Rev. Lett. **83**, 4289 (1999).
[10] R. A. Bartels, A. Paul, H. Green, H. C. Kapteyn, M. M. Murnane, S. Backus, I. P. Christov, Y. Liu, D. Attwood, and C. Jacobsen, Science **297**, 376 (2002).
[11] Z. Zeng, Y. Cheng, X. Song, R. Li, and Z. Xu, Phys. Rev. Lett. **98**, 203901 (2007).
[12] Y. Oishi, M. Kaku, A. Suda, F. Kannari, and K. Midorikawa, Opt. Express **14**, 7230 (2006).
[13] V. S. Yakovlev, M. Ivanov, and F. Krausz, Opt. Express **15**, 15351 (2007).
[14] T. Pfeifer, A. Jullien, M. J. Abel *et al.*, Opt. Express **15**, 17120 (2007).
[15] M. Klaiber, K. Z. Hatsagortsyan, C. Müller, and C. H. Keitel, Opt. Lett. **33**, 411 (2008).
[16] P. B. Corkum, Phys. Rev. Lett. **71**, 1994 (1993).
[17] J. L. Krause, K. J. Schafer, and K. C. Kulander, Phys. Rev. Lett. **68**, 3535 (1992).
[18] K. J. Schafer, B. Yang, L. F. DiMauro, and K. C. Kulander, Phys. Rev. Lett. **70**, 1599 (1993).
[19] K. C. Kulander, K. J. Schafer, and J. L. Krause, in *Superintense Laser-Atom Physics, NATO Advanced Study Institute Series B: Physics*, edited by B. Piraux, A. L'Huillier, and K. Rzazewski (Plenum, New York, 1993), Vol. 316, Chap. 19, p. 95.
[20] M. Lewenstein, P. Balcou, M. Yu. Ivanov, A. L'Huillier, and P. B. Corkum, Phys. Rev. A **49**, 2117 (1994).
[21] E. Goulielmakis, M. Schultze, M. Hofstetter *et al.*, Science **320**, 1614 (2008).
[22] G. Sansone, E. Benedetti, F. Calegari *et al.*, Science **314**, 443 (2006).
[23] J. Mauritsson, J. M. Dahlström, E. Mansten, and T. Fordell, J. Phys. B **42**, 134003 (2009).
[24] J. B. Watson, A. Sanpera, X. Chen, and K. Burnett, Phys. Rev. A **53**, R1962 (1996).
[25] F. I. Gauthey, C. H. Keitel, P. L. Knight, and A. Maquet, Phys. Rev. A **52**, 525 (1995).
[26] A. Sanpera, J. B. Watson, M. Lewenstein, and K. Burnett, Phys. Rev. A **54**, 4320 (1996).
[27] Z. Zhai, R. F. Yu, X. S. Liu, and Y. J. Yang, Phys. Rev. A **78**, 041402(R) (2008).
[28] H. Merdji, M. Kovačev, W. Boutu, P. Salières, F. Vernay, and B. Carré, Phys. Rev. A **74**, 043804 (2006).
[29] P. Antoine, A. L'Huillier, and M. Lewenstein, Phys. Rev. Lett. **77**, 1234 (1996).
[30] W. Hong, P. Lu, W. Cao, P. Lan, and X. Wang, J. Phys. B **40**, 2321 (2007).
[31] Y. Mairesse, A. de Bohan, L. J. Frasinski *et al.*, Science **302**, 1540 (2003).
[32] P. Salières, P. Antoine, A. de Bohan, and M. Lewenstein, Phys. Rev. Lett. **81**, 5544 (1998).
[33] J. J. Carrera and S.-I. Chu, Phys. Rev. A **75**, 033807 (2007).
[34] Y. Xiang, Y. Niu, and S. Gong, Phys. Rev. A **79**, 053419 (2009).
[35] P. C. Li, X. X. Zhou, G. L. Wang, and Z. X. Zhao, Phys. Rev. A **80**, 053825 (2009).
[36] P. Zou, Z. Zeng, Y. Zheng, Y. Lu, P. Liu, R. Li, and Z. Xu, Phys. Rev. A **81**, 033428 (2010).
[37] J. T. Lin and T. F. Jiang, J. Phys. B **32**, 4001 (1999).
[38] P. Antoine, B. Piraux, and A. Maquet, Phys. Rev. A **51**, R1750 (1995).
[39] B. Wang, X. Li, and P. Fu, J. Phys. B **31**, 1961 (1998).
[40] P. Lan, P. Lu, Q. Li, F. Li, W. Hong, and Q. Zhang, Phys. Rev. A **79**, 043413 (2009).